(NASA-CR-120729) EVALUATION OF SEMICONDUCTOR SPECIMENS BY X-RAY ANALYSIS Final Report (Alabama Univ., Huntsville.) 38 p HC $3.75 CSCL 20L

N75-22158

Unclas
G3/76 19246

FINAL REPORT

for NASA Contract NAS8-29650

EVALUATION OF SEMICONDUCTOR SPECIMENS BY X-RAY ANALYSIS

March 1975

SUBMITTED TO: National Aeronautics and Space Administration
George C. Marshall Space Flight Center
Marshall Space Flight Center, AL 35812

BY: H. U. Walter
Department of Physics
The University of Alabama in Huntsville
Huntsville, AL 35807

TABLE OF CONTENTS

I. INTRODUCTION

The effort that is summarized in the following was carried out in support of NASA's crystal growth program, and, in particular, in support of Skylab experiments M-555 on Epitaxial Growth of GaAs, M-556 on Growth of CeSe and SeTe Single Crystals by Vapor Transport Reactions and M-560 on Containerless Growth of InSb. A variety of samples was analyzed in support of ongoing research at SSL as well. Germanium and GaAs crystals were investigated for studies on photovoltaic effects, chemical etching and epitaxial growth.

According to the overall objective to assess the defect structure of single crystalline materials, the X-ray facility that was set up under this contract allows for Laue diffraction studies including modifications thereof such as microbeam Laue and large area Laue topography, Schulz and Berg-Barrett topography (modified optical spectrometer), scanning Lang, Berg-Barrett and Borrman topography (AMR topographical camera) as well as diffractometer studies.*

Hardware has been described in earlier reports; a crystal wafering saw for cutting of precisely oriented crystals was also designed and constructed.

In the following, a brief survey of basic theory and topographical techniques is provided; examples of topographs are presented.

---

*Powder and rotating crystal cameras are also available.

II. THEORY

Investigation of crystal imperfections by X-ray diffraction techniques is based on the fact that Laue diffraction spots have a fine structure that reflects the structural perfection of the crystal under investigation. X-ray topographical techniques record intensity diffracted from large areas of a crystal at high resolution. Recorded images reflect the overall geometry and single crystallinity of a sample, black and white images of defects are superimposed on the general background. For thin crystals where the product of linear absorption coefficient μ and thickness t is less than 1 or for back-reflection images, defects appear primarily as darker features on a photographic emulsion. For thicker samples, where $\mu t > 10$, light images are obtained. Samples with intermediate thickness may show both, light and dark images of defects. Densities of dislocations up to the order of $10^4/cm^2$ can be resolved, beyond this point topographical techniques are of little use due to overlap of dislocation images.

In terms of kinematic theory, image contrast formation in X-ray topographs due to strain fields in crystals can be explained as follows: Intrinsic reflection ranges can be calculated for perfect crystals. As an example, half width for [220] Bragg reflections for the case of symmetrical transmission and negligible absorption is for silicon 1.7 sec. of arc for Ag $K\alpha_1$ and 5.5 sec. for Cu $K\alpha_1$, for germanium 3.8 sec for Ag $K\alpha_1$ and 15 sec. for Cu $K\alpha_1$ radiation. Primary beam divergence usually is of the order of minutes ($< \Delta\theta_{1-2}$) and only a small fraction of the intensity will be diffracted by defect-free material. In case of strain fields modifying the periodicity of the lattice, a larger

divergence will be accepted for diffraction and the additional intensity will result in direct images of defects. Similar considerations apply for wavelength spread.

Considering absorption, the direct image intensity decreases according to:

$$I = I_o \cdot \ell^{-\mu_o t} \qquad (\mu_o \equiv \text{linear absorption coefficient}, \; t = \text{thickness})$$

Accordingly, direct image topographs correspond to the thin crystal case, $t \lesssim 1$. If recorded on photographic emulsions, defects or strained regions show up as black images on grey background, similarly the integrated intensity for a mosaic crystal is higher than for a perfect crystal. Since the strain fields surrounding dislocations are anisotropic, direction of Burgers vectors can be determined by determining diffraction planes that exhibit maximum and minimum image contrast. As an example, minimum contrast for screw dislocations is obtained if $\vec{g} \cdot \vec{b} = 0$, maximum contrast if $\vec{g} \parallel \vec{b}$.

In kinematical or geometric theory, the assumption is made that the amplitude of X-rays incident on all the diffraction centers of the crystal is the same, thus neglecting the amplitude diffracted by previous layers of the crystal. This is only valid for crystals made of mosaics of thin crystallites or, more generally speaking, very imperfect crystals. When studying diffraction by a thick, perfect crystal, one has to take into account all the interactions between the incident and diffracted waves and the crystal. Dynamical theory considers these interactions and image contrast formation especially with perfect crystals as well as some other diffraction phenomena that can be observed on topographs

can only be understood in terms of dynamical theory. For basic information, a selected bibliography is given in the appendix. A basic treatment of dynamical theory would be beyond the scope of this report, however, some specific phenomena that are due to dynamical effects are mentioned briefly in the following.

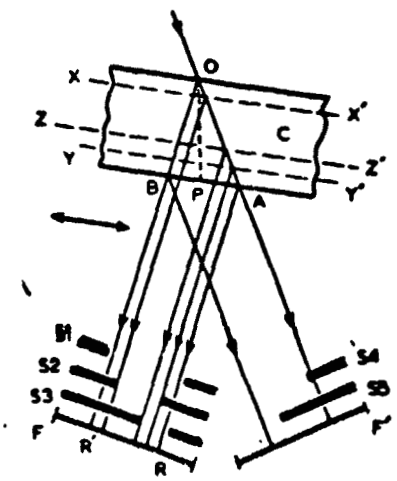

Fig. 1. Arrangements for "limited projection topographs" and "direct beam topographs".

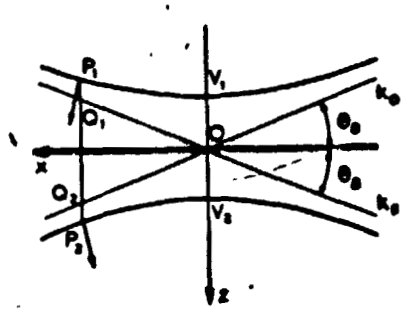

Fig. 2. Dispersion surface in vicinity of Brillouin zone boundary.

One of these phenomena, "margin enhancement," can be observed with section topographs of perfect, weakly absorbing samples. Fig. 1 gives the path of rays for limited projection topographs. Fig. 2 is a sketch of the dispersion surface and of the asymptotic surfaces of the wave vectors in the crystal, $\vec{k}_o$ and $\vec{k}_g$, in the vicinity of the Brillouin zone boundary. Oz lies in the Brillouin zone boundary and is directed toward the center of the crystal in the direction $\vec{k}_o + \vec{k}_g$.

The intensity profile of the diffracted beam is - for nonabsorbing crystal - described by the following equation:

$$I_p = \text{Const } (1 - p^2)^{1/2}$$

where

$$p = \frac{W}{\sqrt{1 + w^2}} ,$$

$$W = 2X \tan \theta_B / D$$

$$D = \overline{V_1 V_2} \approx \frac{e^2}{mc^2} \frac{F\lambda C}{\pi V \cos \theta_B}$$

W is the so-called deviation parameter which is linearly proportional to the deviation, $\Delta\theta$, from the exact value of the Bragg angle, D is the distance $\overline{V_1 \ V_2}$ (see Fig. 2) expressed in terms of F ≡ structure factor, V ≡ volume of the unit cell, C ≡ polarization factor (C = 1 for O polarization, C = $|\cos 2\theta|$ for 180° polarization state). If there is only a small departure from the symmetrical Laue case such as indicated in Fig. 1, the section topograph intensity profile across the image RR' will differ very little from the above relation for the intensity

variation. Its form is that of the curve $\mu t = 0$ on the right half of Fig. 3. On the left side, intensity profiles are given for the transmitted beam as they would be recorded along TT' in Fig. 1. These curves for non-zero absorption apply to X-ray reflections with which the Borrman

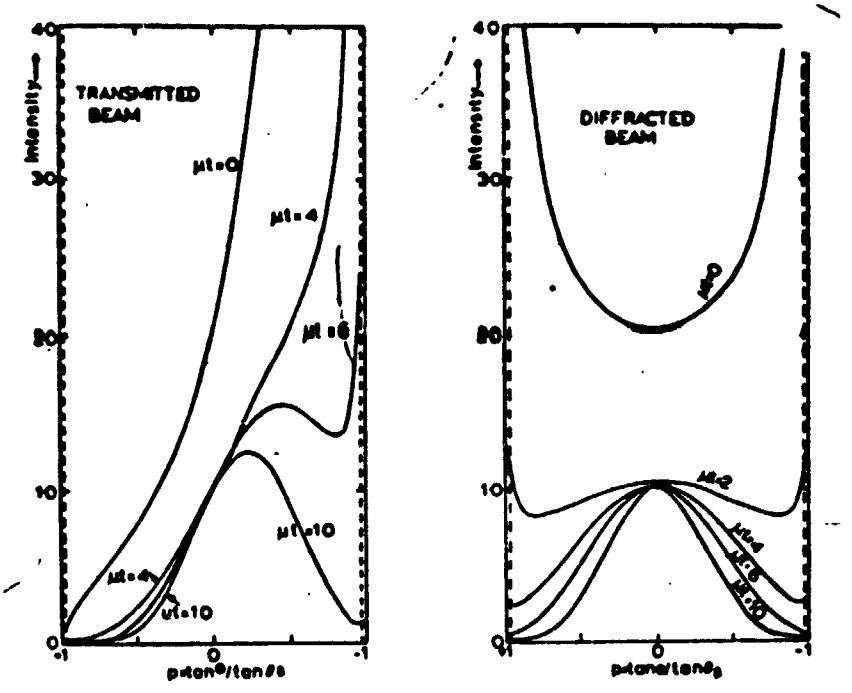

Fig. 3. Calculated spatial intensity profiles for section topographs of diffracted beam and direct beam.

effect can strongly develop, such as (220) in diamond structure. It can be seen that the margin enhancement is rapidly attenuated with increasing thickness, it has practically disappeared at $\mu t = 2$.

Another phenomenon that can be observed in topographs which also reflects dynamical scattering are Pendellösung fringes. These fringes can be observed with topographs of bevelled crystals. The spacing corresponds to the extinction distance $E = 1/D$, where $D = V_1 V_2$ in Fig. 2. For silicon, (220) reflections, MoKα radiation, this distance is about 35 μm. For a crystal plate of thickness t the integrated

reflection R as a function of t is given by

$$R = \frac{1}{2} \pi \, Dd \int_0^{2\pi tD} I_o(x) \, dx.$$

A plot of R versus tD for the first oscillations is shown in Fig. 4.

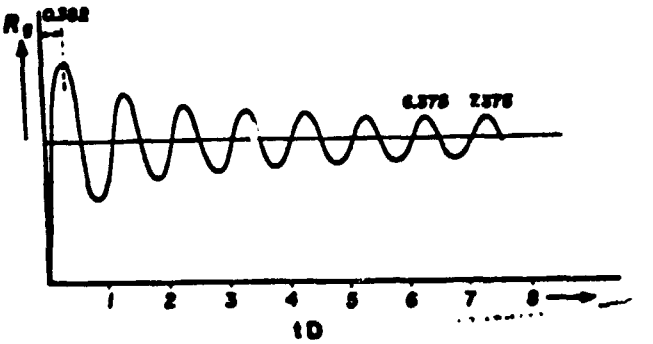

Fig. 4. Variation of integrated reflection with crystal thickness, perfect crystal, zero absorption.

The intensity and hence visibility on topographs decays proportionally to $(tD)^{-1/2}$. Since Pendellösung fringes can be observed with highly perfect crystals only, fringe visibility provides a statistical measure of lattice perfection that is sensitive to lattice imperfections too small to be resolved individually on topographs. Margin enhancement can be used in a very similar manner for assessment of crystal perfection.

Multiple reflections and interactions may lead to standing wave patterns within the crystal. Since absorption is to a very great extent due to interaction with electrons, standing waves with nodes between the atoms (β-branch waves) are absorbed, whereas waves with nodes at the position of the atoms (α-branch waves) pass through the crystal with extremely low absorption. Since the α-branch wave has a forward-diffracted beam component as well as a diffracted beam component, the

diffracted-direction anomalously transmitted wave for a thick crystal is at most 1/8 of the incident beam intensity. Borrman topographs make use of this "anomalous" transmission effect for investigating crystal perfection. If a local strain field such as caused by dislocation is present, absorption takes place. As a result, defects cast shadows, the Borrman shadow, and are visible as areas of lesser X-ray intensity on the photographic emulsion (white images). This type of topograph is obtained with $\mu t > 10$, samples with intermediate thickness, $1 < \mu t < 10$, generally show both, white images due to destruction of Borrman effect as well as black images due to kinematic effects.

III. BRIEF SURVEY OF TOPOGRAPHICAL TECHNIQUES

X-ray topographic techniques produce an image of a surface by [illegible] or cutting a crystal, or of the projection of a selected volume of crystal, by recording the diffracted X-ray intensity issuing from such surface or volume. Diffracted X-ray intensity is usually recorded with photographic emulsions; other possibilities include the use of counters or image converters. Intensity variations of radiation diffracted from crystals that are oriented with respect to the incident beam such that constructive interference results according to Bragg's law is due to either orientation contrast or extinction contrast. Orientation contrast is due to lattice misorientations, contrast arising from point-to-point variations in lattice perfection (strain fields) is usually termed "extinction" contrast.

Important experimental variables include wavelength spread of the radiation, the degree of collimation of the incident beam and geometrical arrangements to insure resolution and imaging of larger samples.

Methods that Apply White Radiation

One of the least critical topographical methods, large area Laue topography, is simply a modification of the Laue diffraction technique that is commonly employed for crystal orientation. Instead of having a small diameter beam (usually 1 mm), a much larger beam diameter of the order of sample size is used. Transmission or back reflection topographs can be obtained. Information concerning twin and grain boundaries or single and polycrystallinity can be obtained (see Section IV).

Closely related to the above technique is the Schulz technique where again continuous radiation from a point source is used. Back reflection is used rather exclusively, usually several Laue spots are produced (see Section IV). With microfocus tubes, single dislocations can be resolved.

The basic advantage of white radiation techniques is their simplicity. Samples can be poly - or single crystalline; there is no need to orient the sample with precision in order to satisfy the Bragg condition for a particular wavelength. Disadvantages are due to overlapping of images and only fair angular and spatial resolution. To overcome these limitations, characteristic radiation techniques are applied.

Characteristic Radiation Methods

Absorption filters are used with the following topographical techniques:

Berg-Barrett technique: This technique which was developed by Berg in 1931 and improved by Barrett in 1945 is the most widely used topographical technique. Special effort is made with this technique to have relatively large source to specimen and small specimen to film distance so that good resolution is obtained. The first images of dislocations were observed by Newkirk using this technique. Under favorable conditions, the photographic plate may be set so that it is no further than a fraction of a millimeter apart from the specimen surface illuminated by X-ray and spatial resolution of a few μ can be obtained. Undistorted topographs can be obtained so that one to one correlation with the actual sample can be made (see Section IV).

Surface reflection techniques that employ rocking or simultaneous scanning of film plus sample have been reported by Wooster and Merlini and Guinier. Large samples can be investigated with these techniques while good resolution is retained.

If information on bulk properties is to be obtained, transmission techniques are used. For resolution of a few microns, well collimated primary beams are required. Consequently, only a small section of a sample is illuminated and recorded (section topographs). For investigation of large samples, moving specimen and moving film techniques are used. With the Lang technique sample and film are traversed simultaneously so that a map of large samples can be obtained. (Projection topographs).

Arrangements similar to the Lang technique can be used with methods that employ anomalous transmission (Borrmann effect). Only highly perfect crystals can be studied.

With double-crystal methods collimation and monochromatization is achieved by Bragg reflection from a highly perfect monochromator crystal. Surface reflection or transmission topographs can be obtained.

The facility that was set up under this contract allows studies by the following techniques:

1.) Laue diffraction techniques

2.) Schulz technique

3.) Berg-Barrett technique

4.) Lang and Borrman technique

5.) Diffractometer techniques

Double crystal rocking curves have also been recorded using a germanium monochromator crystal. Mechanical stability of the system and accuracy of angular settings of the monochromator was, however, marginal.

IV. EXPERIMENTAL RESULTS AND APPLICATIONS

A very large number of topographs and diffraction images were obtained during the course of this work. Only some representative examples that illustrate applications are presented in the following. Hardware and experimental considerations such as selection and processing of emulsions have been covered in previous reports, references for further information are given in the appendix.

It should be noted that intensities are reversed with all topographs shown. Light areas on the prints correspond to areas of higher intensity of diffracted radiation.

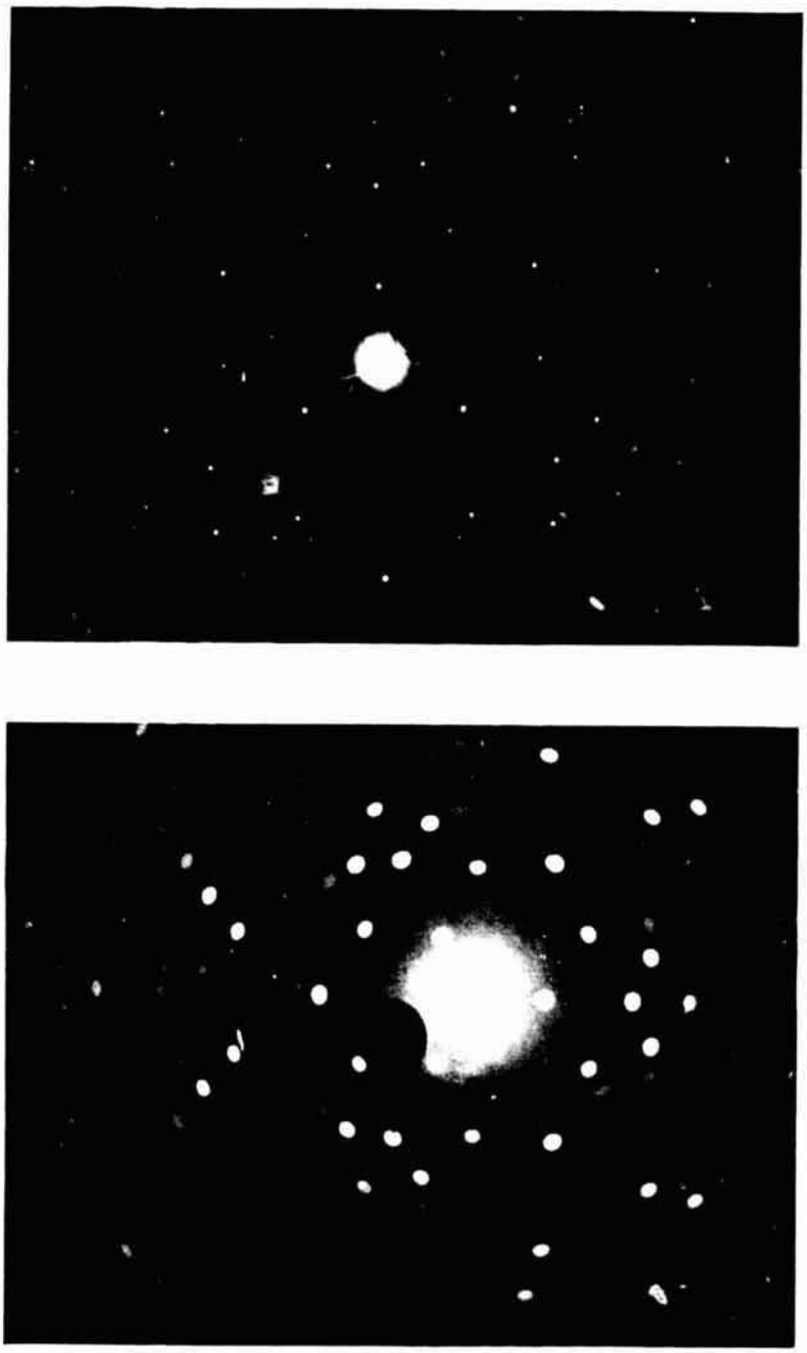

Fig. 1. Laue diffraction patterns of Si(111), transmission, 0.5 mm and 2 mm dia. beam. The small beam diameter is particularly useful for probing of small areas or grains and for precision orientation of single crystals.

Fig. 2. Laue back reflection from space processed (M-556) germanium selenide, (001).

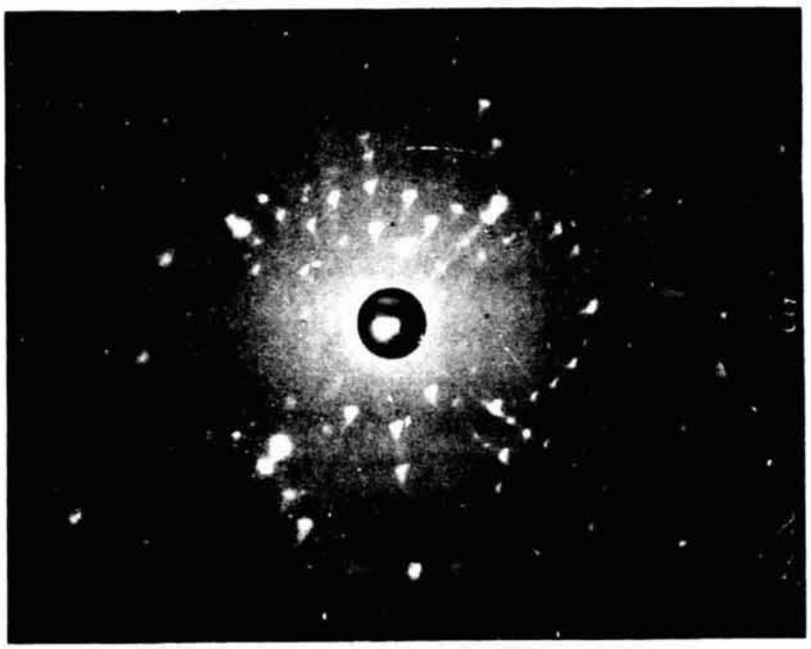

Fig. 3. Same sample as in Fig. 2, transmission. Both diffraction patterns indicate that the sample is strained and consists of several grains. Plastic deformation during reentry or damage introduced by handling could be the cause.

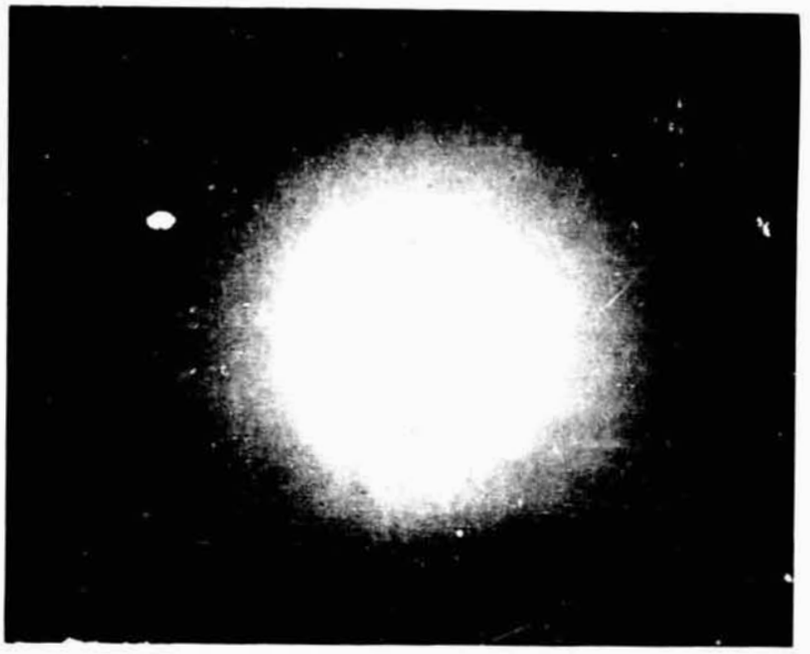

Fig. 4. Laue back reflection obtained from space-grown germanium selenide (M-556). A multitude of slightly misoriented grains contributes to the general (001) diffraction pattern

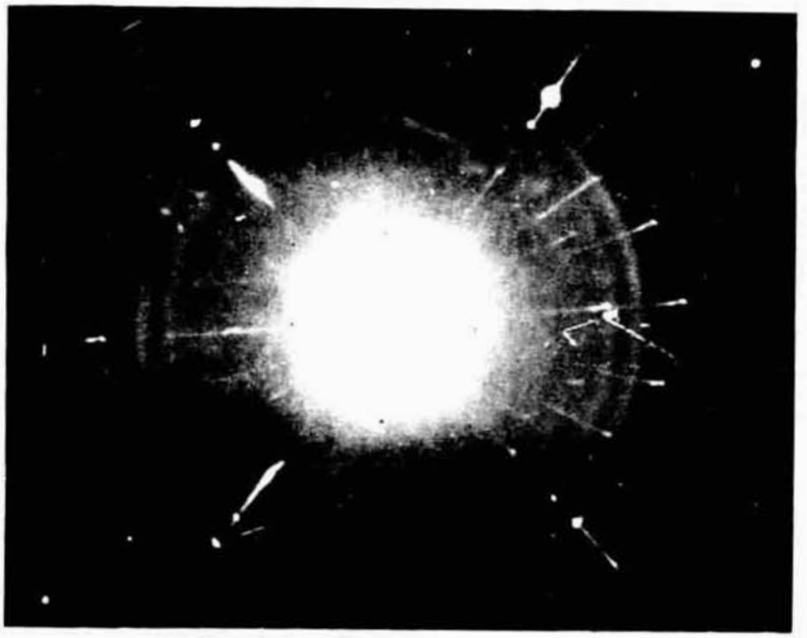

Fig. 5. Same sample as in Fig. 4, transmission. Again, multiple grains are evident. Debye-Scherrer rings may be due to polycrystalline precipitates on sample surface.

Fig. 6. Si(111), transmission large area Laue topographs. Indices can be assigned to these reflections as is commonly done with Laue diffractions by stereographic projection techniques. Laue topographs as shown in this figure are basically equivalent to Schulz topographs as shown in Figs. 7, 8, and 9.

Fig. 7. Schulz topograph of InBi(001), continuous Cu radiation.

Fig. 8. Schulz topograph of InBi(001), continuous Cu radiation.

Fig. 9. Schulz topograph of InBi(001), magnification of one large reflection. Inclusions, cracks and strain fields due to compositional variations are clearly visible.

Fig. 10: [333] Berg-Barrett topograph, static exposure, of (111)-oriented germanium wafer. Experimental simplicity of the techniques where scanning is eliminated while good resolution is retained make this approach attractive, a major shortcoming is that image width can only be as large as the focal length of the X-ray line source. This is usually of the order of 1 cm and only the center section of this wafer could be imaged. Fig. 11 shows a topograph of the same crystal, scanning was used and a complete image is obtained.

Fig. 11. Germanium (111) - [333] Berg-Barrett topograph. For this reflection 2θ is approximately 90° and, consequently, undistorted high resolution images can be obtained.

Fig. 12. GaAS (100), Westinghouse sample # E-2, [400] Berg-Barrett topograph. Sample consists of two grains, and has many inclusions or cavities.

Fig. 13. GaAs(100), Westinghouse sample #W-2. [400] Berg-Barrett topograph. Wafer is warped at left bottom corner, a dense network of dislocation can be seen; beam divergence too large, therefore, both Kα, and $K\alpha_2$ images visible.

Fig. 14. GaAs(111), [333] Berg-Barrett topograph. Large grains, strain fields and dislocations can be seen.

Fig. 15. GaAs(111), [333] Berg-Barrett topograph. Large grain, strain fields and dislocations can be seen.

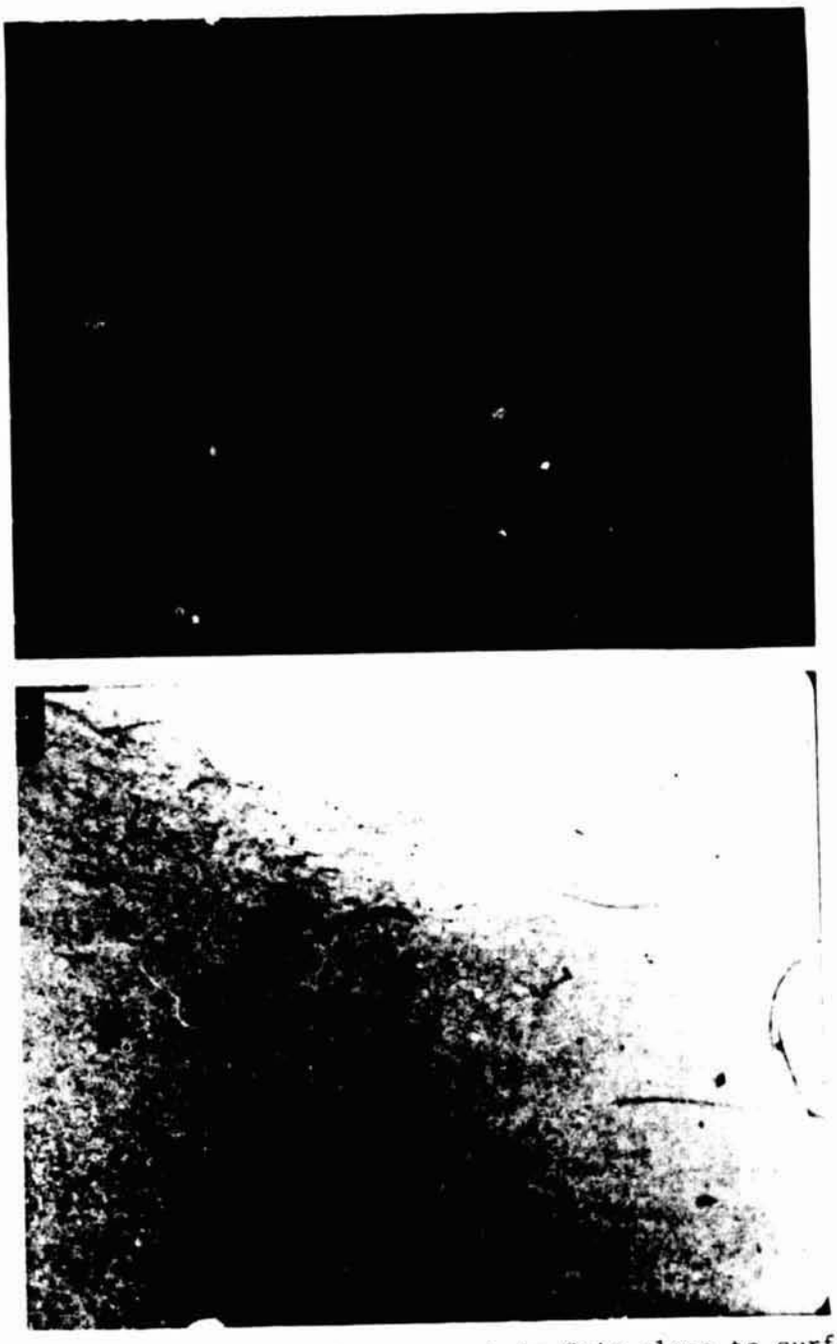

Fig. 16. Examples of dislocation network in GaAs close to surface (back reflection topographs).

Fig. 17. Precipitates due to oxygen in silicon. [220] Lang transmission topograph of (111) wafer, Cu K_α radiation.

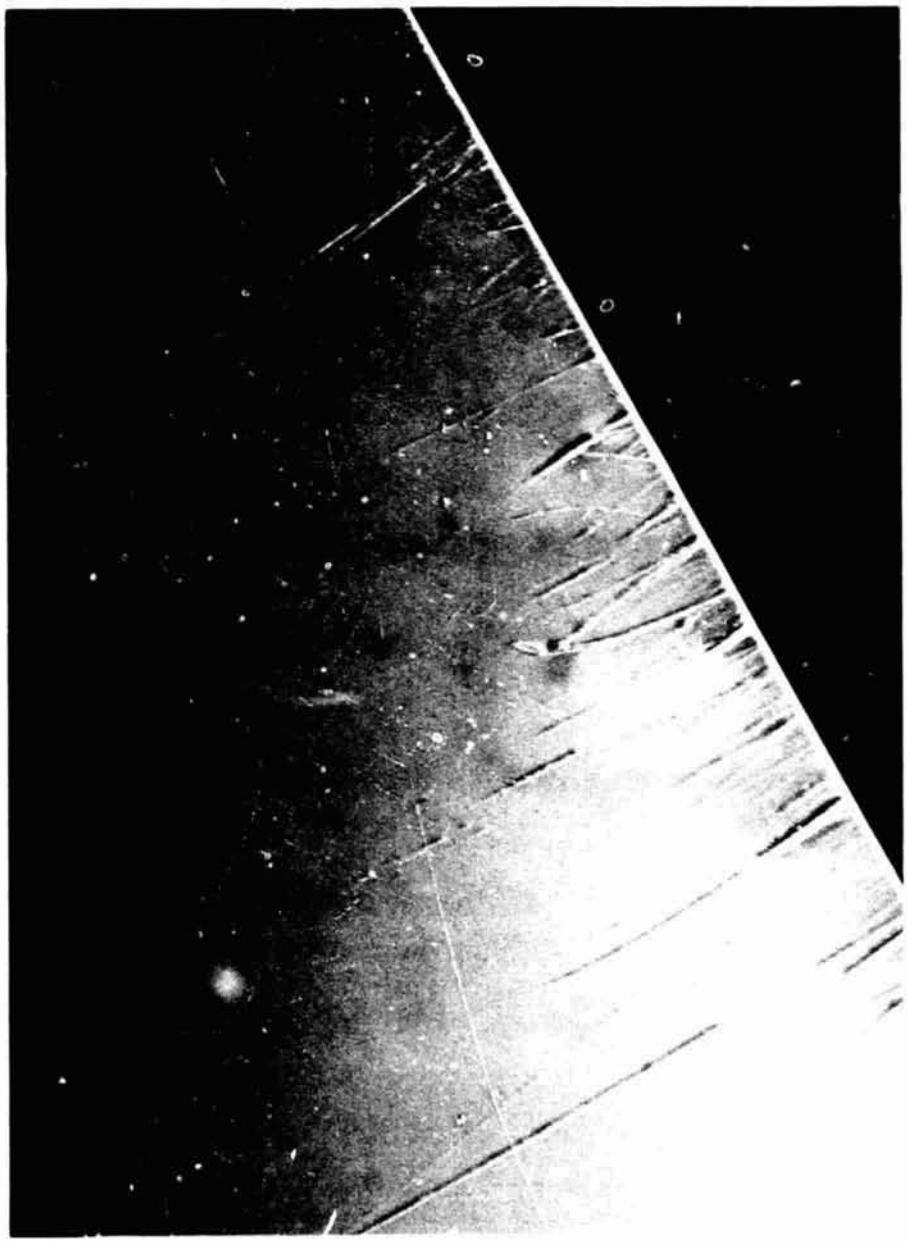

Fig. 18. Dislocation and slip lines in silicon. [220] Lang transmission topograph of (111) wafer, Cu Kα radiation.

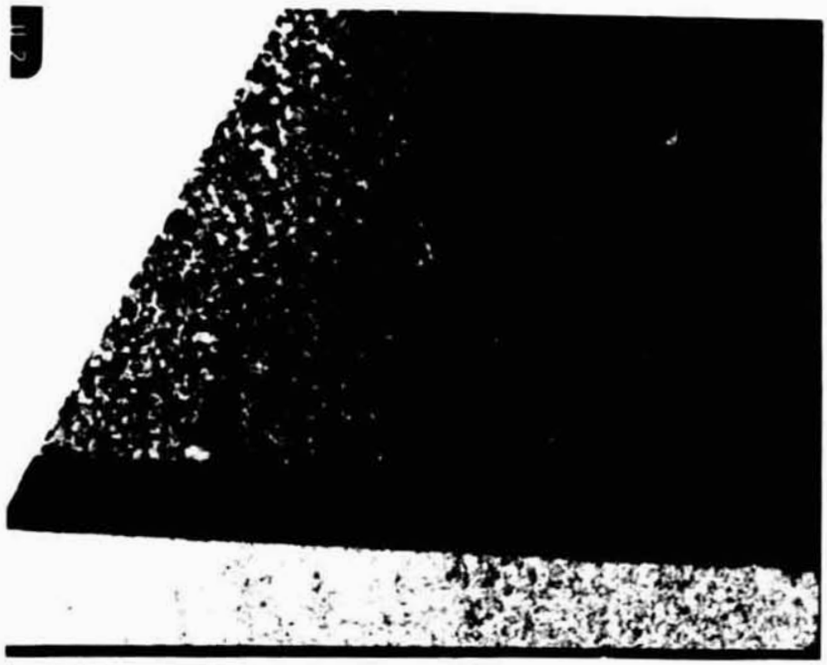

Fig. 19. Precipitates in silicon, 56x magnification.

Fig. 20. Dislocation lines in silicon, 56x.

Fig. 21. InSb, M-560, [220] surface reflection topograph of as-grown crystal.

Fig. 22. InSb(110), M-560. [220] reflection topograph, Cu Kα radiation.

Fig. 23. InSb(110), M-560. [220] reflection topograph, Cu Kα radiation.

Fig. 24. InSb(Se), M-560, (111) - [220] Borrman topograph. Dislocation network and outgrowing mechanism of dislocations is clearly visible (growth direction from bottom to top).

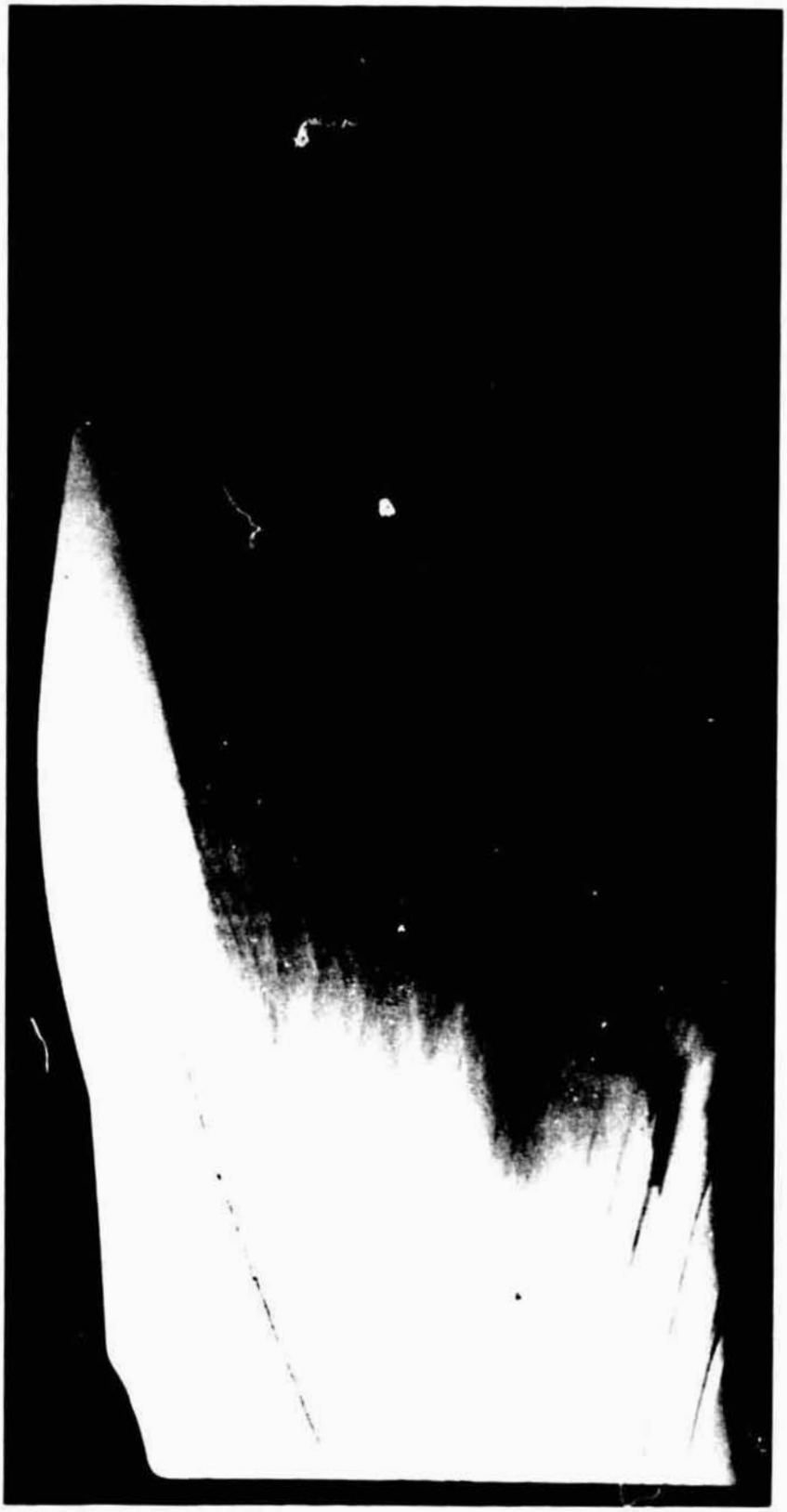

Fig. 25. [333] reflection topograph of InSb wafer shown in Fig. 24. Again, dislocations and decrease in density of dislocations as growth proceeds is clearly visible. Faint intensity variations due to variation of selenium concentration can also be discerned at top of sample.

BIBLIOGRAPHY

The following bibliography is intended to provide some introductory background information:

L. V. Azaroff: Elements of X-ray Crytallography, McGraw Hill 1968.

R. F. Bunshah, editor: Techniques of Metals Research, Vol. II, Techniques for the Direct Observation of Structure and Imperfections. J. Wiley 1969.

E. Maieran: The Application of X-Ray Topographical Techniques to the Study of Semiconductor Crystals and Devices, Siemens Report 1969.

A. R. Lang: Modern Diffraction and Imaging Techniques in Materials Science. North Holland Publ. Co. 1969.

B. W. Batterman, H. Cole: Rev. Mod. Phys. 36 (1964) 681.

A. Guinier X-ray Diffraction in Crystals, Imperfect Crystals, and Amorphous Bodies, W. H. Freeman and Co. 1963

A. Rachandran: Advanced Methods of Crystallography, Academic Press 1964

J. Auleytner: X-Ray Methods in the Study of Defects in Single Crystals, Pergamon Press 1967

A. Guinier: X-Ray Crystallographic Technology, Uilger and Watts LTD 1952.